ANALYSIS OF LEADING EDGE AND TRAILING EDGE COVER GLASS SAMPLES BEFORE AND AFTER TREATMENT WITH ADVANCED SATELLITE CONTAMINATION REMOVAL TECHNIQUES

S.P. Hotaling
Rome Laboratory, OCPC
Griffiss Air Force Base, New York 13441-5700

ABSTRACT

Two samples from Long Duration Exposure Facility (LDEF) experiment M0003-4 were analyzed for molecular and particulate contamination prior to and following treatment with advanced satellite contamination removal techniques (CO_2 gas/solid jet spray and oxygen ion beam). The pre- and post-cleaning measurements and analyses will be presented. The jet spray removed particulates in seconds. The low-energy reactive oxygen ion beam removed 5,000 Å of photo polymerized organic hydrocarbon contamination in less than 1 hour. Spectroscopic analytical techniques were applied to the analysis of cleaning efficiency including: Fourier transform infrared, Auger, x-ray photoemission, energy dispersive x ray, and ultraviolet/visible. The results of this work suggest that the contamination studied here was due to spacecraft self contamination enhanced by atomic oxygen plasma dynamics and solar UV radiation. These results also suggest the efficacy for the jet spray and ion beam contamination control technologies for spacecraft optical surfaces.

INTRODUCTION

Today, satellite contamination is kept within specification during production, assembly, and storage by clean rooms, solvent wipes, inert gas/air purges, and vacuum bakeout. Although these techniques have proven acceptable for launching "clean" satellites (level 1000 typical), the combined effects of the space environment lead to increased contamination levels once deployed (ref. 1,2). LDEF was initially launched with MIL-STD-1246B Level 2000C cleanliness. This is considered clean by industry standards today, but post-recovery LDEF analysis showed over 1 lb of molecular contaminants notwithstanding particulates (ref. 3). LDEF experiments provide a unique window into the contamination effects on a large variety of spacecraft materials, all exposed to the same low-Earth orbit (LEO) environment for the same amount of time. Thus, LDEF really is a "treasure trove of data" as described by S.A. Little in 1991 (ref. 4).

In this paper, the results of utilizing the CO_2 jet spray and oxygen ion beam contamination removal techniques for the cleaning of LDEF contaminant species will be discussed. The overall conclusion of the paper is as follows: Indeed the proper choice of spacecraft materials and prelaunch cleanliness is important, but the physical realities of the space environment necessitate an on-orbit contamination mitigation philosophy which is potentially implementable using the contamination control techniques described herein.

PRECEDING PAGE BLANK NOT FILMED

PRECLEANING SAMPLE ANALYSIS

Optical microscopy was used to obtain sample morphological features. EDX, Auger, ESCA, and FT-IR were used to obtain chemical and compositional information. UV/Vis spectrophotometry provided the optical properties for the samples. Computer image analysis was utilized to analyze the microscopy data. After contamination removal, the same techniques were applied to the samples (ref. 5).

Two solar cell cover glass samples from the LDEF experiment M0003-4 were analyzed in this study. Sample No. L3-IV-4-14-52 was positioned on LDEF tray D9 on the leading edge of the spacecraft. Sample No. T3-IV-4-14-54 was positioned on the trailing edge of the spacecraft in tray D3. The leading edge sample (henceforth, sample L) was visually different in appearance than the trailing edge sample (henceforth, sample T).

Sample L collected 5,000 Å of an organic contaminant film, scattered particulate debris, and two micrometeorite craters. Circular polarized optical microscopy showed the presence of many orders of brightly colored Newton's interference rings on sample L, as shown in Figure 1 (magnification = 13×). This figure is a montage of micrographs pasted together in a jigsaw puzzle fashion since the field of view for one micrograph at 13× was too small to contain the entire sample. Seen here are the two halves of the sample placed together. The cover glass sample was stuck to the silicon backing plate by the contaminant film which acted like an adhesive. This afforded the opportunity to analyze the effects of this photo-polymerized contaminant and contamination removal techniques on both the cover glass and crystalline silicon materials. Subsequent microscopic analysis revealed the presence of a subsurface fracture running across the crystalline silicon sample. This defect was deemed responsible for the sample becoming severed in the analysis procedure.

Sample T on the other hand collected only 50 Å of a light brown contaminant film and scattered particulate debris. This sample was not "glued" to its silicon backing plate. Sample L was in two parts, as can be seen from close examination of Figure 1. As discussed above, sample T was not found to be as heavily contaminated as sample L, and was not fixed to its crystalline silicon backing plate. In Figure 2, sample T is positioned above square graph paper (20 squares per inch). From this figure, the thin brown contaminant film is clearly seen as a contrast difference.

The physical condition of these samples was anti-intuitive. Since the leading edge sample experienced a higher atomic oxygen (AO) fluence than the trailing edge of the spacecraft (ref. 6), one would expect a fairly clean-contaminant free surface. It is possible that such a surface would even be slightly eroded due to interaction with the reactive flux. During recovery, the AO fluence for sample L was 8.74×10^{21} atoms-cm^{-2}. The trailing edge sample was somewhat shielded from this AO flux, having an AO fluence of 1.3×10^{17} atoms-cm^{-2}. Intuitively, the author expects this to imply a thicker contaminant deposition on the trailing edge relative to the leading edges, which was not the case for the two samples examined in this work. The author is still speculating as to the reasons for this contamination density inversion.

FT-IR spectroscopy was performed with a Biorad FTS-40 spectrophotometer. The FT-IR spectrum of the contaminant film taken from sample L's interferences fringes on the silicon side of the sample is shown in Figure 3. Figures 4a and 4b show that the FT-IR spectrum of nylon 6:6 is present in

the contaminant film. Another expansion of the hydrocarbon region for the sample is shown in Figure 5a. In Figure 5b, the FT-IR spectrum of polyacetal Delrin 500 plastic is shown. Figures 4 and 5, when correlated with Figure 3, indicated that the major constituents of the contaminant film are nylon 6:6 and Delrin 500.

ESCA and Auger microprobe analyses were performed at several points in and around the micrometeorite crater shown in Figure 6. The seven numbered positions in Figure 6 indicate the Auger microprobe beam positions. The Auger electron spectrum for the crater is shown in Figure 7. The seven sampling positions did not offer strikingly different data for chemical proportion. The chemical composition of the film is given in Table 2.1 as atomic percentages. The atomic percentage values calculated from the Auger spectra were commensurate with those calculated from ESCA, giving confidence in the identification of the chemical composition of the contaminant.

A lower magnification view of the micrometeorite crater of Figure 6 is shown in the SEM photo of Figure 8. In Figure 8, the interference fringes are clearly visible as dark bands. The SEM photo of Figure 8 indicates that some of the contaminant film is starting to peel off the substrate, as can be seen by the small area of film at about 2 o'clock referenced from center, the position of the micrometeorite crater (see arrow). Also clear in this figure are several pieces of particulate ranging in size from 0.2 mm down to probably the tens of microns spatial dimension. EDX analysis of these particles identified them as mostly metallic: copper, zinc, tin, aluminum, and silicon.

CONTAMINATION REMOVAL

Gas/Solid Jet Spray Technique

The gas/solid jet spray was used to remove particulate contamination. The CO_2 jet spray is shown in Figure 9. The jet spray has been described in the literature (ref. 1, 2), but may be simply described as a particle removal process which exploits momentum transfer from incident snow flakes to particulates adhering to the surface through van der Waal's forces (first and second order). The energy/momentum transferred to the adhered particle breaks these surface potential forces, and the "free" particle is entrained in the gas stream and carried away from the surface. The mixture of solid/gas in this process is very important for the removal of submicron particles (ref. 1), which are not removed by high pressure gas and liquid streams due to the gas/surface boundary layer's "insulating" action.

Ion Beam Technique

The molecular film was removed by reactive ion etching using a beam of oxygen ions and electrons from a Hughes helicon wave source (HWS) shown in Figure 10. The output beam contains oxygen ions and neutral atoms as well as electrons. The HWS also has a UV radiation component. The effects of these species upon contaminant removal is under investigation. The ion cleaning experimental parameters are as follows. The ion energy was varied between 12 and 45 eV (average). The ion flux densities varied between 550 and 1,300 $\mu A/cm^2$ (average) as measured by a Faraday cup. The plasma was operated at 165 mHz with a power of 10 to 20 W. The oxygen flow rate was measured to be 10 sccm using an Omega Engineering gas flow meter (FMA-5601). Chamber partial pressures were monitored by

a VG Scientific Micromass 560 mass spectrometer to be: oxygen, 3×10^{-5} torr; water, 3×10^{-5} torr; and nitrogen, 5×10^{-5} torr. Other species were present in the chamber registering partial pressures of less than 1×10^{-8} torr, and, as such, were of no consequence to this work.

POSTCLEANING SAMPLE ANALYSIS

Figure 11 shows a circular polarized light micrograph of a heavily contaminated region of sample L. The region of the sample to the left of the circular arc (AB) was masked while the region to the right of the arc was exposed to 1 hour of reactive oxygen ions. Comparison with Figure 1 shows that the sample was cleaned by the reactive oxygen ion beam. Figure 12 is a Nomarski photomicrograph (200×) of the region surrounding the crater before ion beam treatment. The same region at the same microscopic settings is shown in Figure 12 after ion cleaning. Note that only the outline of the crater remains and that the contaminant film has been completely removed. The jet spray removed the particular debris, including the particles of glass chips on glass substrate.*

In 1 hour of total treatment time, the sample went from being contaminated at levels that the unaided eye could easily discern, to having a contamination level at the Nomarski microscopy threshold of detection.

Figure 14 is a fluorescence light micrograph of a masked and unmasked section of sample L after 21 minutes of ion beam cleaning. The dark (nonfluorescing) side of the micrograph shows the result of removal of 1,760 Å of molecular film. There is evidence of residual contamination (brightly fluorescing yellow matter) near the mask boundary.

The brown film of sample T (see Fig. 2) was removed with 5 minutes of reactive oxygen ions. The UV/Vis spectra for the sample before and after ion cleaning are shown in Figure 15. A UV/Vis spectrum of the very edge of the sample, which was masked during the LDEF flight and ion cleaning operations, was taken. Comparison of the spectra corresponding to this protected edge and the ion cleaned area of the sample showed conclusively that the sample was completely cleaned, within optical detection limits.

CONTAMINATION COLLECTION

The above contamination removal techniques have been shown to successfully remove spacecraft contamination, and development is underway to build small, lightweight flight qualifiable contamination removal systems. However, there remains the problem of preventing the removed contaminants

*It is well known that removal of glass chips from glass substrates after long periods of time is a most difficult problem. Additionally, there is evidence of variations in humidity of the LDEF environment during the (post STS-landing) ferry flights (ref. 3). This implies that not only did the glass chips fall on a glass surface, but that the presence of post-flight humidity enhances the probability for a very strong glass to water chemical bond which would be a very tenacious particle to remove. Of course, the interfacial geometry is very important for the removal, but it is noteworthy that not only metallic and fibrous particulates were removed by the jet spray, but also glass chips from a glass surface.

from redepositing onto the cleaned surfaces. In response to this, Rome Laboratory developed a contamination collection device. This contamination collector is capable of collecting and containing both molecular and particular contaminants throughout the spacecraft operational parameter space (temperature, vibration, radiation, vacuum, and micrometeorite environments). One embodiment of this device, the Aerogel Mesh Contamination Collector (AMCC, patent pending) is shown in the SEM of Figure 16. In the figure is shown a cross section of the AMCC with collected particulate contaminants of various sizes. In a system, the AMCC would work in conjunction with the jet spray and ion beam removal devices as shown in Figure 17. Here, the reactive ion beam removes organic particles and molecular films as the jet spray removes particles and entrails the removed species into the AMCC's waiting pores (ref. 1, 2).

CONTAMINATION CONTROL FOR SPACECRAFT APPLICATIONS

The above contamination removal techniques are being developed for autonomous operation in spacecraft applications. These data present the first results of the application of these contamination mitigation technologies to long-duration spacecraft exterior surface materials. The cleaning rates and efficiencies obtained are optimistic. This suggests further contamination control experimentation in orbital systems such as the retrievable payload carrier (RPC), as shown in Figure 18 (ref. 7). In such an experiment, small jet spray and ion beam sources would be mounted in a pallet which could be reused for both leading edge and trailing edge missions, and/or several low-cost contamination control pallets could be fabricated and flown on several RPC missions in various locations. RPC contamination experiment data would fuel a contamination control system for Space Station *Freedom.*

ACKNOWLEDGMENT

The author wishes to thank Barry Lippey and Dan Demeo of Hughes Aircraft Corporation for their kind hospitality and research collaboration on the contamination removal phase of this work. The author also wishes to thank Maurice Dumais of USAF/Rome Laboratory (Hanscom AFB) for his hospitality in the performance of the electron microscopy work. The hospitality and expertise of N.T. Castello of Oneida Research Corporation are greatly appreciated. The effort could not have been funded without the ardent support of Capt. Deidra A. Dykeman, Rome Laboratory Contamination Control Program Manager. The author wishes to thank Terry Trumble of USAF/Wright Laboratory for providing the samples used for the experiment.

REFERENCES

1. Hotaling, S.P., and Dykeman, D.A.: "An Advanced Particle Removal and Collection System." To appear in *Particles on Surfaces IV*, K. Mittal (ed.), Plenum Press, 1993.

2. Hotaling, S.P., and Dykeman, D.A.: "An Introduction to Rome Laboratory Contamination Control Technology," RL-TM-92-18, 1992.

3. Crutcher, E.R., et al.: Proceedings of the First LDEF Post-Retrieval Symposium, A.S. Levine (ed.), NSA CP-3134, 1991, pp. 101, 121, 141, 155, 847, and 861.

4. Little, S.A.: "The Role of the LDEF in the Development of Space Systems," p. 1687.

5. Hotaling, S.P.: "The Application of Jet Spray and Ion Beam Contamination Removal Techniques to Samples From the LDEF Spacecraft." To appear in Proc. High Power Optical Components Conf., NIST, 1993.

6. Bourassa, R.J., and Gillis, J.R.: "LDEF Atomic Oxygen Flux and Fluence Calculations." Boeing LDEF task NAS1-18224, Task 12 Report, January 1991.

7. Perry, A.T.: "Retrievable Payload Carrier—Next Generation LDEF." In Proc. First LDEF Post-Retrieval Symposium, A.S. Levine (ed.), NASA CP-3134, 1991, p. 1698.

Figure 1. Montage of photomicrographs (magnification: 13×) taken with circular polarized light. The thick contaminant film is indicated by the presence of several orders of Newtonian interference rings. The area defined by the "crescent moon" shape on the left side of the circle is the cover glass on top of a crystalline silicon backing plate. The contaminant film is on the top surface of the cover glass and also deposited between the cover glass and the silicon backing plate. The region to the right of the glass is the crystalline backing plate with associated contamination. It is also noteworthy that the center of the sample shows indication of a micrometeorite impact. The white rectangular area in the upper left of the figure is a "missing piece" which somehow was not photo-documented.

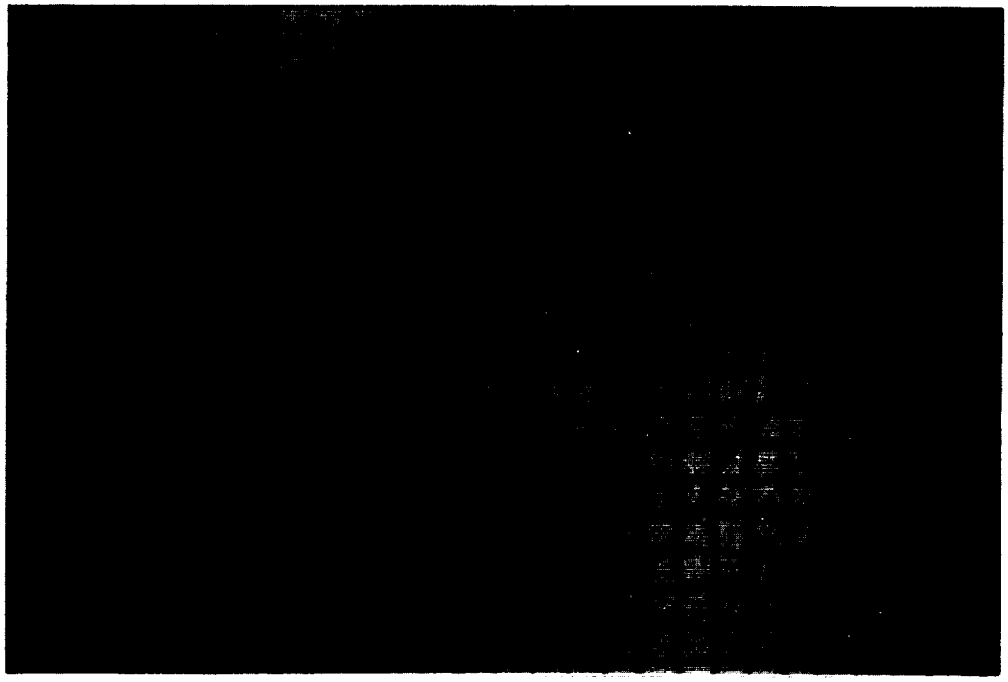

Figure 2. The trailing edge sample viewed with circular polarized light at a magnification of 3×. The sample is positioned over a piece of graph paper (20×20 squares/inch). The contaminant film on this sample is apparent as a brown stain which is not uniform in thickness. Note the vast difference in appearance of the contaminant films in Figures 1 and 2.

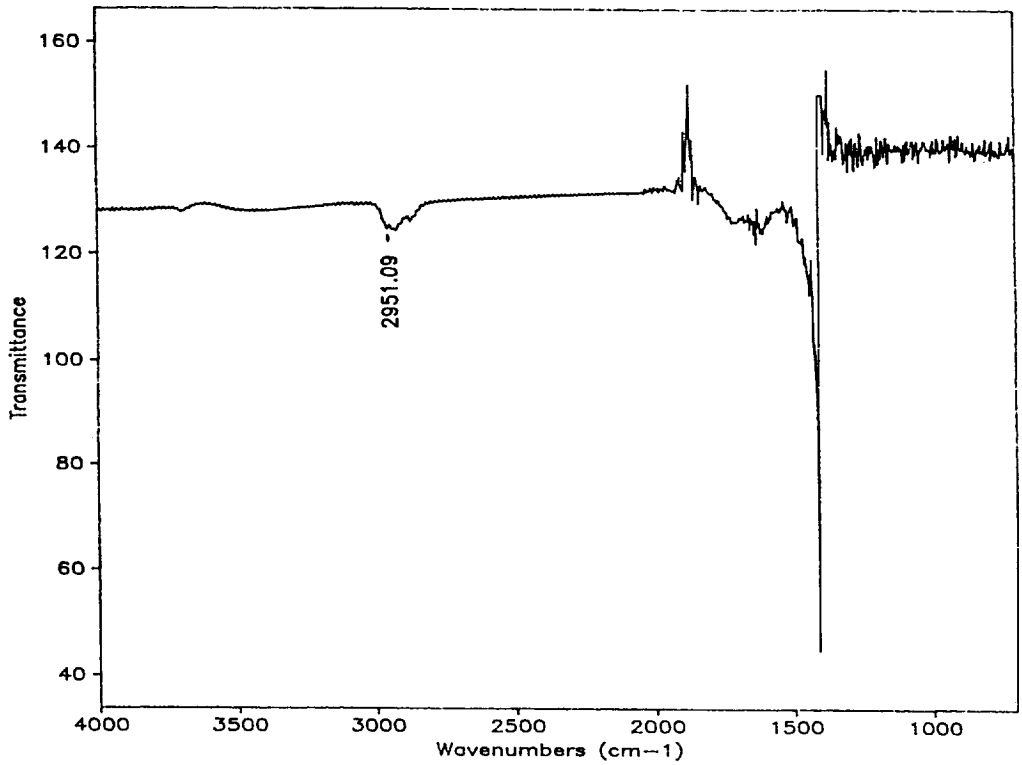

Figure 3. The FT-IR spectrum (reflection mode) of the contaminant film of Figure 1. The figure indicates the absorption region which was associated with aliphatic hydrocarbons.

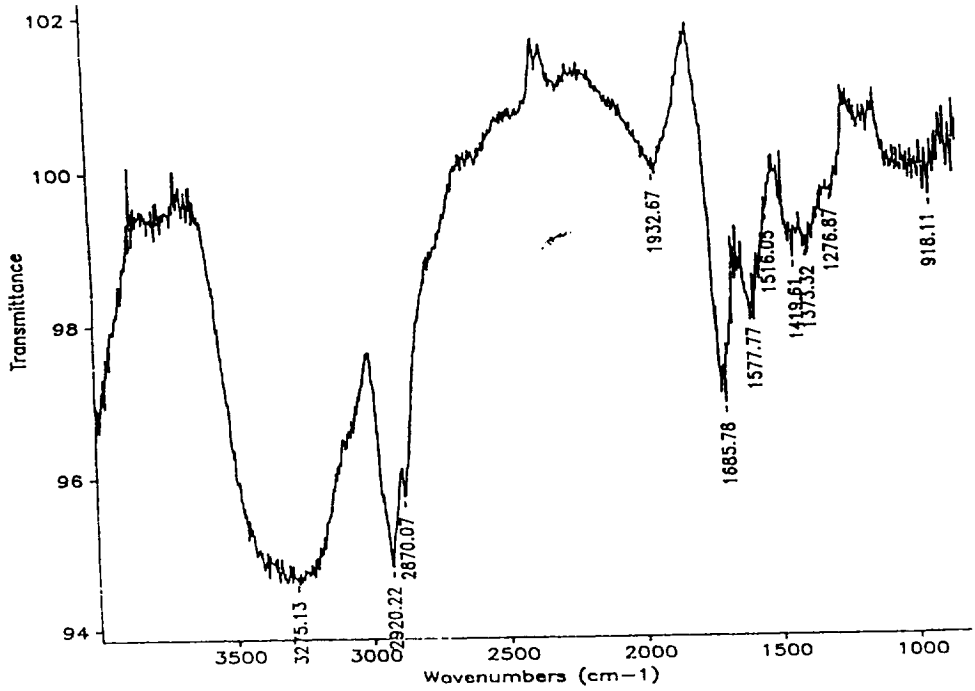

Figure 4*a*. An expansion of the hydrocarbon region of the FT-IR spectrum of Figure 3.

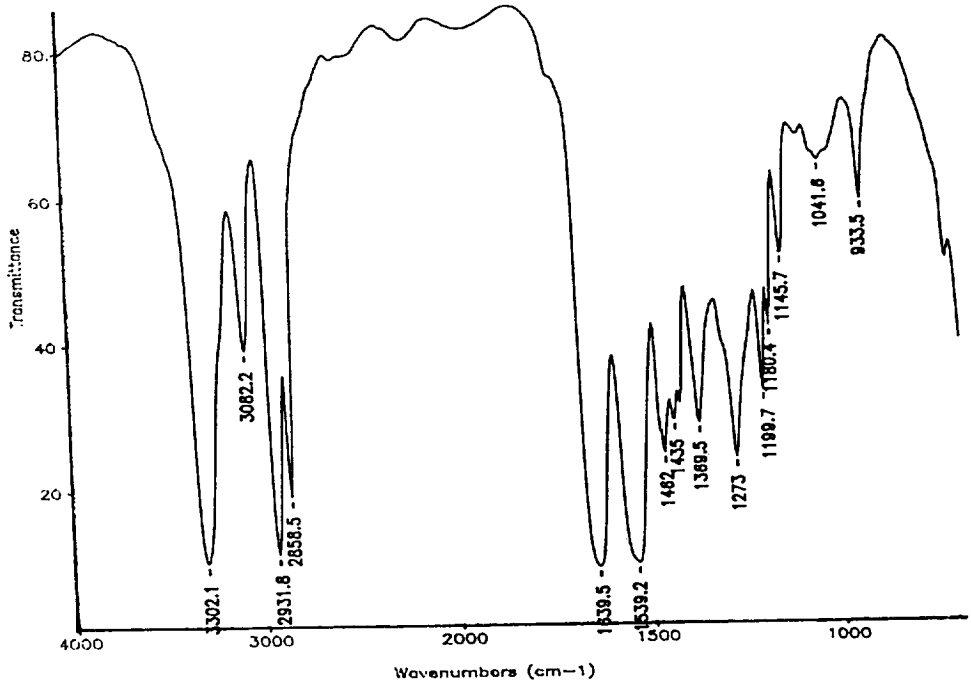

Figure 4*b*. The FT-IR spectrum of nylon 6:6 which is correlated with Figure 4*a*.

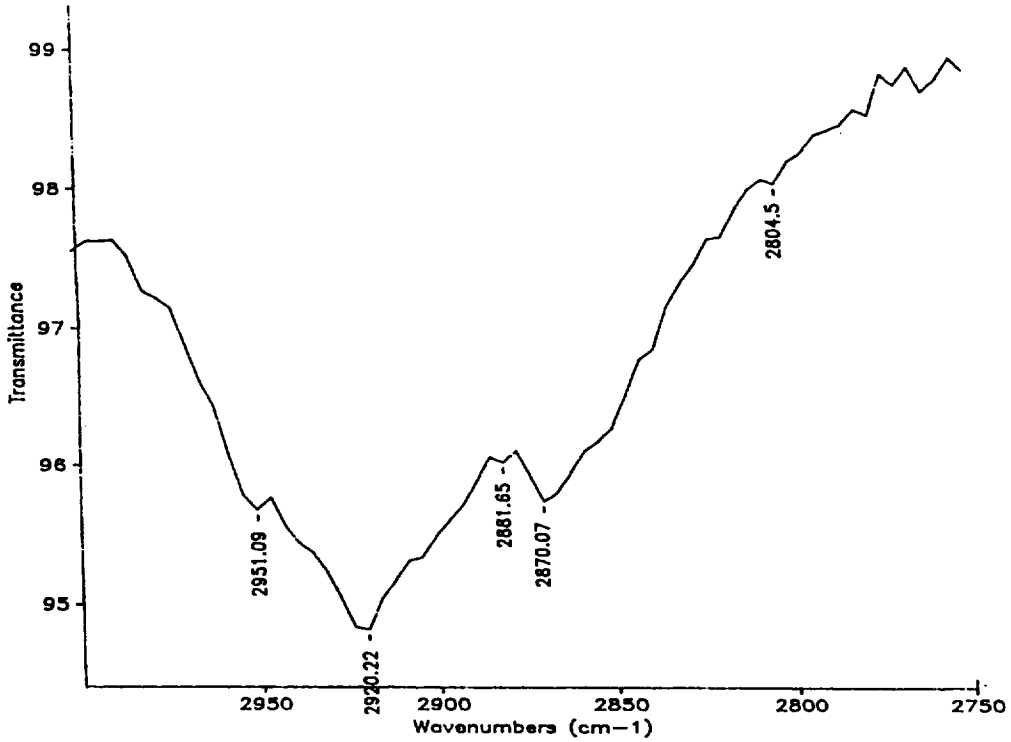

Figure 5*a*. An expansion of the hydrocarbon spectrum of Figure 3.

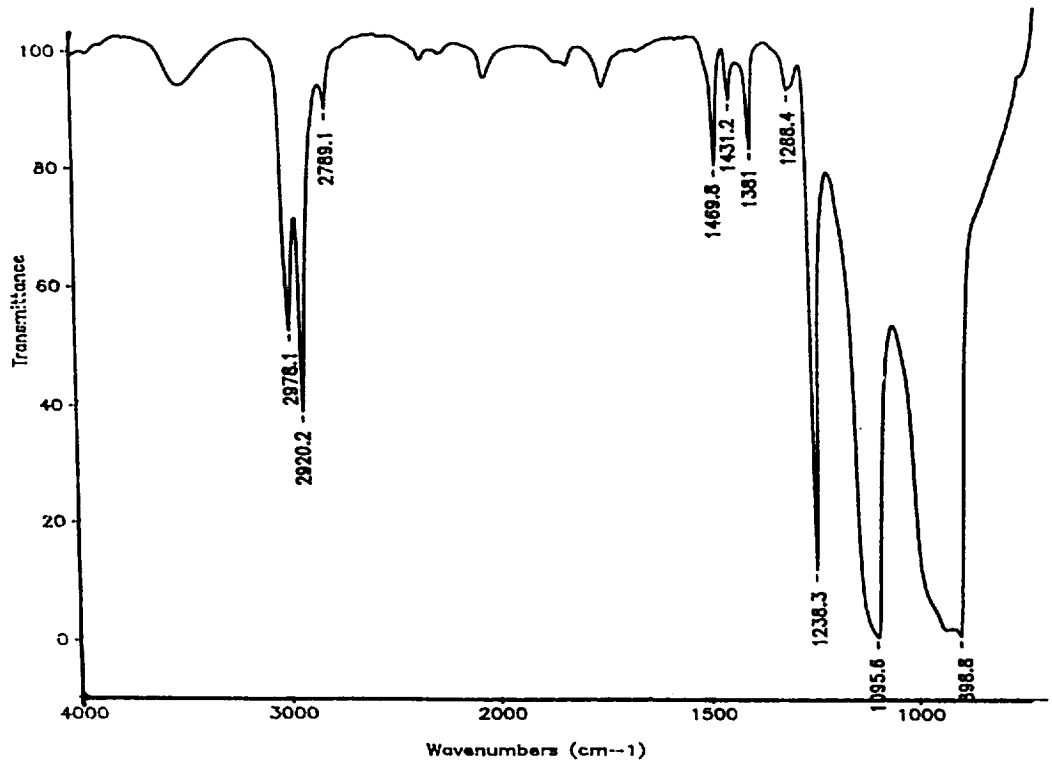

Figure 5*b*. The FT-IR spectrum of polyacetal Delrin plastic which correlates with Figure 5*a*.

Figure 6. A SEM photo of the micrometeorite (or artificial space debris) impact site in the center of Figure 1. The seven numbered sites indicate positions of the Auger microprobe analysis.

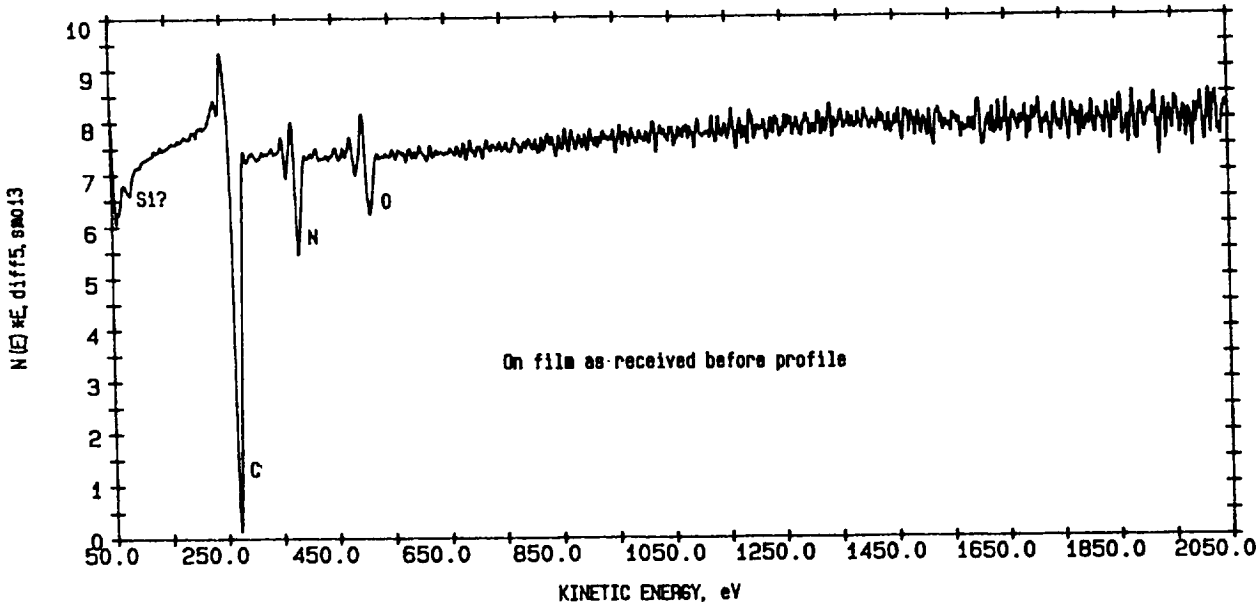

Figure 7. The Auger electron spectrum (AES) from location number 1 of Figure 6. These AES data were typical of those of Figure 6 locations; differences were in magnitude of the Auger peaks only.

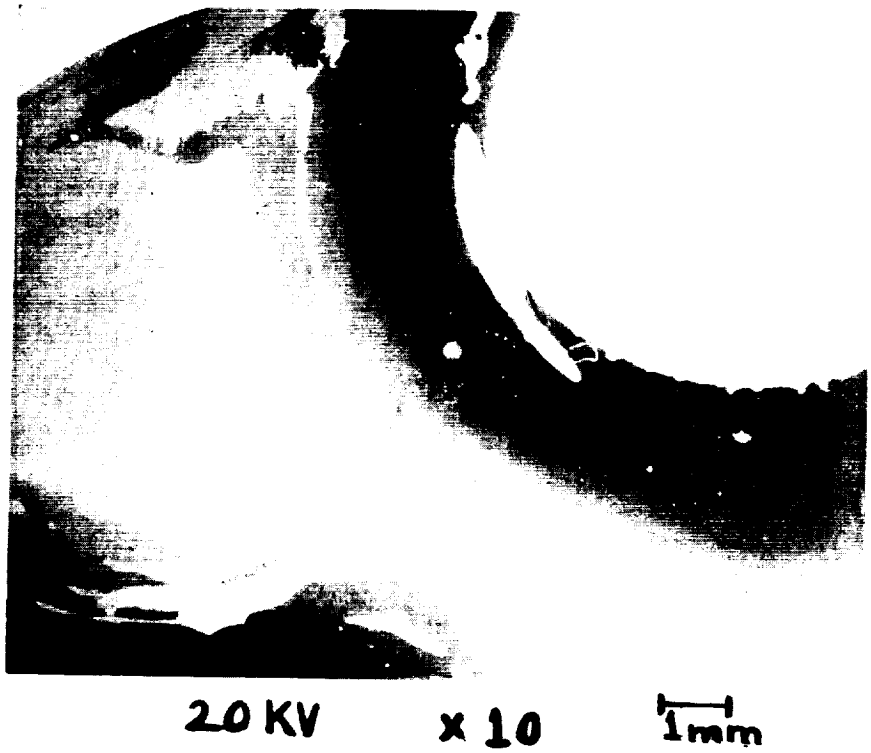

Figure 8. A low magnification (10×) SEM photo of the leading edge sample showing the central micrometeorite crater illustrated in Figures 1 and 8. Note the scattered particulate debris and shadowing of one of the areas of the contaminant film. This shadow is believed to be the start of film delamination.

Figure 9. A 35-mm photograph of a research model CO_2 gas/solid jet spray in operation. Newer designs are much smaller and more compact. Flight units have been designed and are awaiting production.

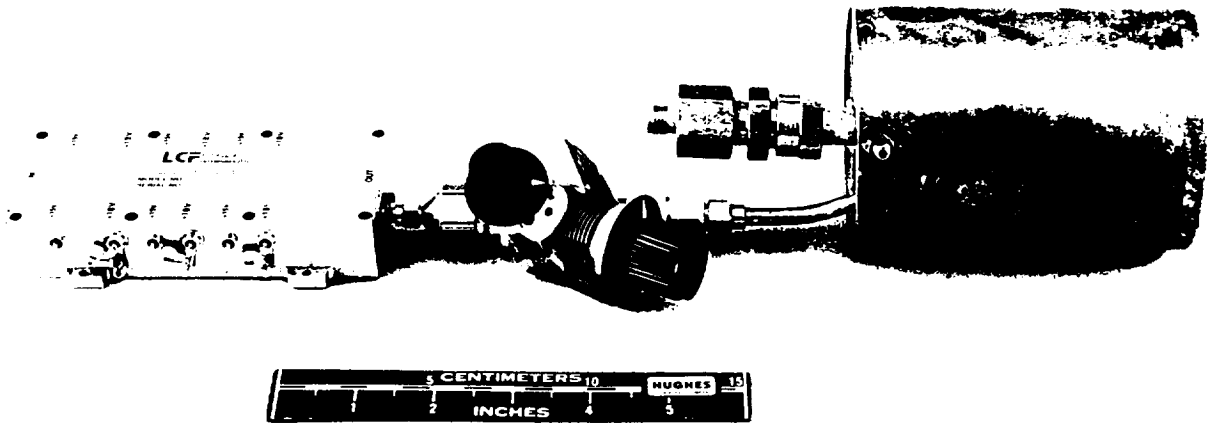

Figure 10. A 35-mm photograph of an old research model HWS ion beam cleaner. The newer designs are inductively coupled, obviating the variable capacitors between the RF amp and cavity, and is much smaller and more lightweight.

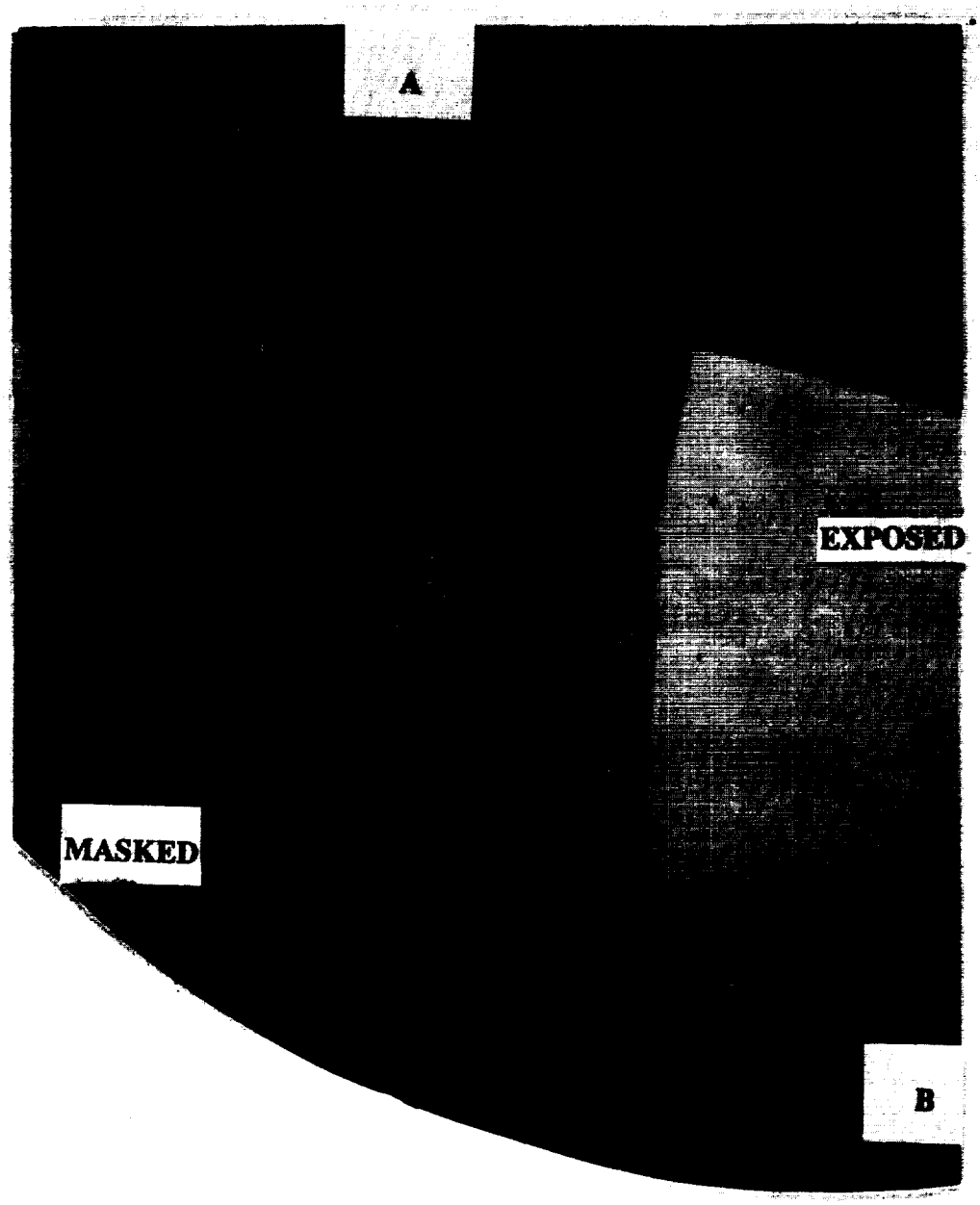

Figure 11. A circular polarized light micrograph (13×) of a section of the leading edge sample after treatment with the ion beam and jet spray contamination removal devices. The region to the left of the circular arc was also exposed to the cleaning treatments while the glass coverslip masked (protected) the contamination. This Figure thus illustrates a before/after type comparison for the cleaning techniques. The sample was treated with 1 hour of reactive oxygen ion cleaning.

Figure 12. A Nomarski light micrograph (magnification: 200×) of the leading edge sample prior to treatment with contamination removal techniques. The brightly colored interference rings indicate a thickness of 4,500 Å of contaminant film. Notice also the presence of scattered secondary debris and other particular contamination absorbed onto the sample surface.

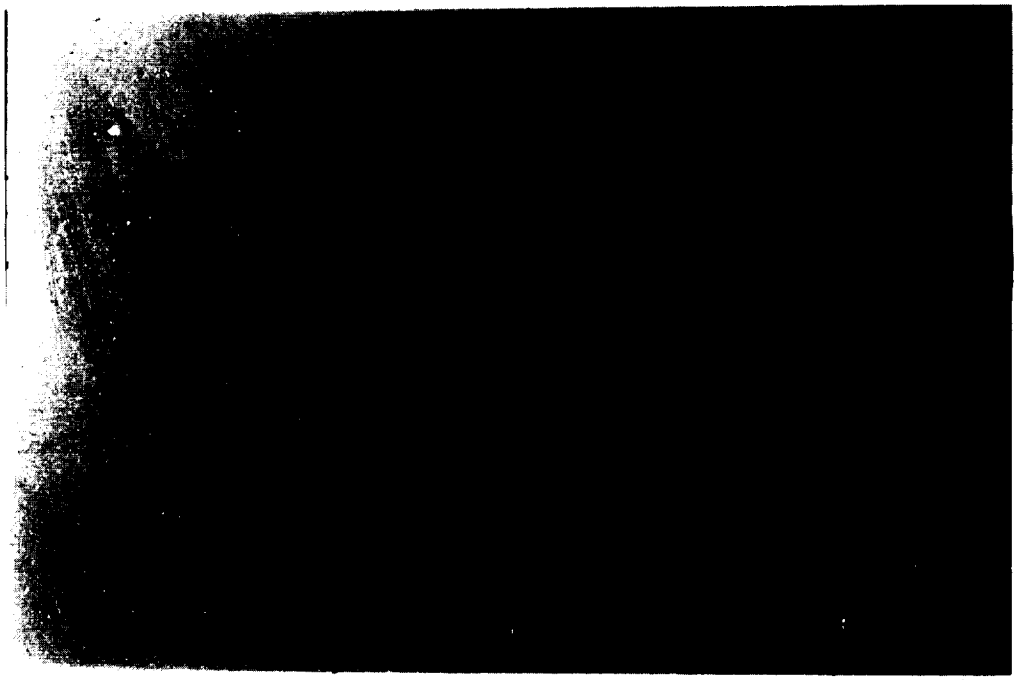

Figure 13. A Nomarski photomicrograph (magnification: 200×) of the micrometeorite impact region of Figure 12 after treatment with the gas/solid jet spray and ion beam cleaners. There is only a faint indication of the presence of residual film. Nomarski gives an approximate thickness less than 15 Å. Note also that most of the particular debris has been removed.

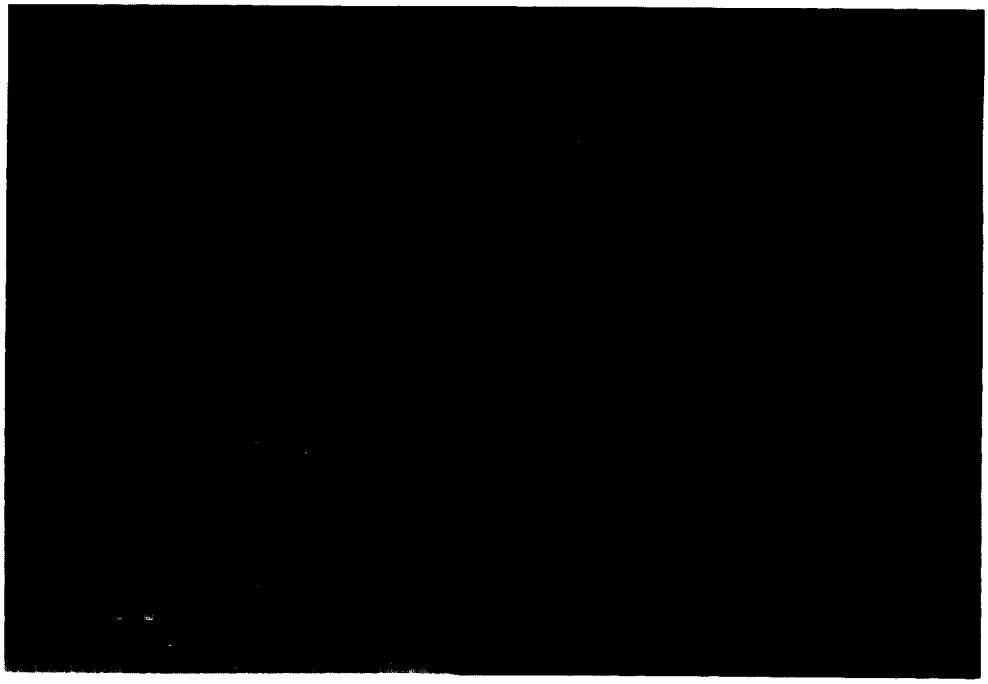

Figure 14. A blue light fluorescence light micrograph of the cleaned (dark)/uncleaned (bright yellow and green) section of the leading edge sample. As in Figure 11, the cover glass masked (protected) part of the sample from cleaning treatments. This sample was treated with 21 minutes of reactive oxygen cleaning.

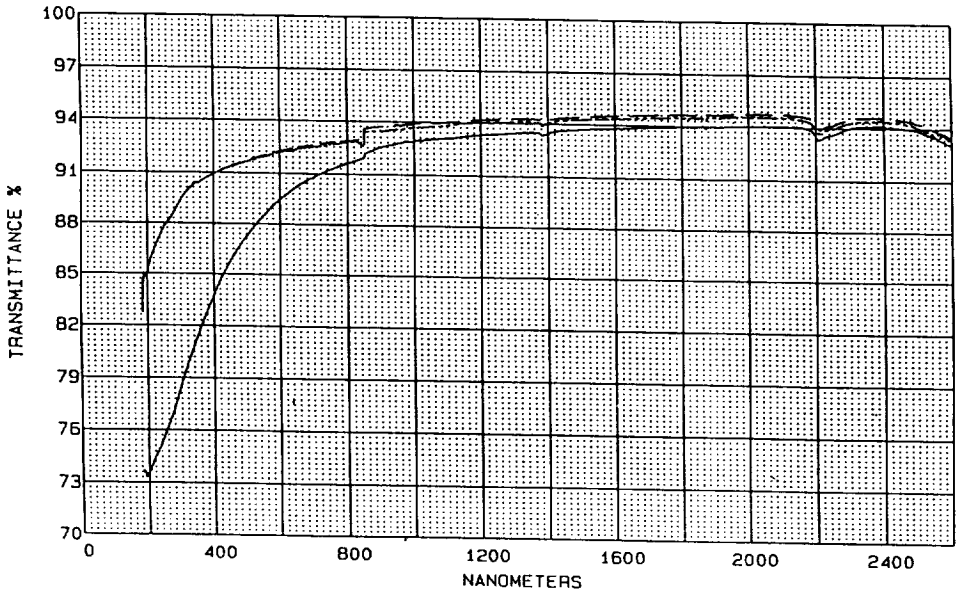

Figure 15. The ultraviolet/visible (UV/Vis) transmission spectra for the trailing edge sample before (solid) and after (dashed) treatment with the ion cleaner. The after cleaning spectrum of a section of the sample which was protected from direct interaction with the space environment was compared to that of the sample after ion cleaning. No difference was discernible, indicating that the cleaning was highly efficient.

Figure 16. A SEM photo of the Aerogel Mesh Contamination Collector (AMCC, patent pending) showing captured particles.

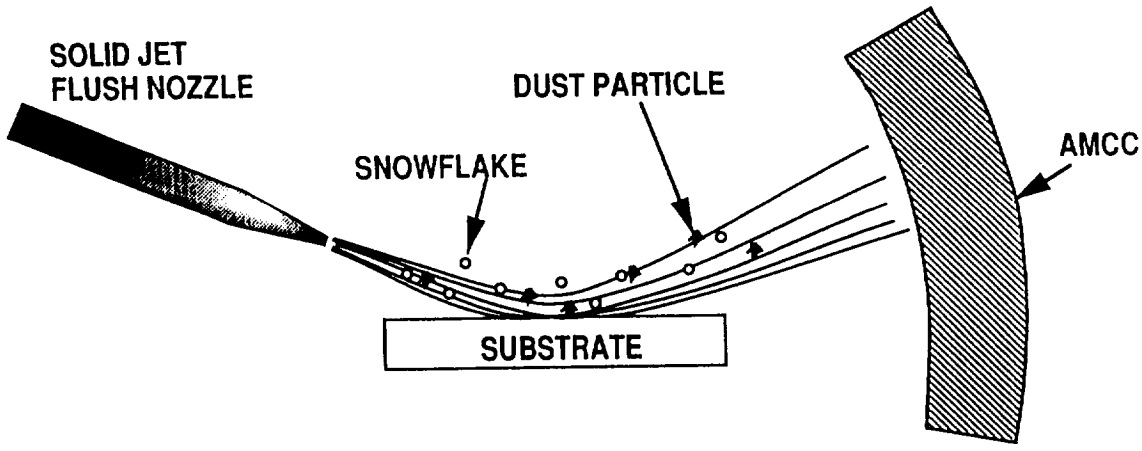

Figure 17. A system concept level diagram of the jet spray and AMCC in operation.

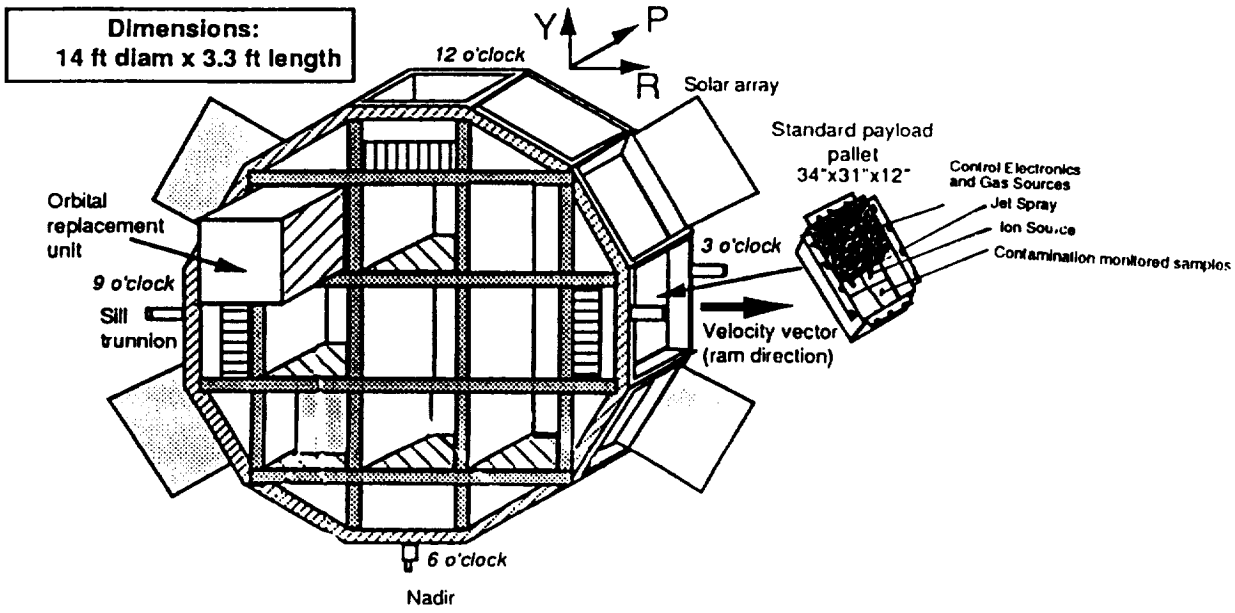

Figure 18. A concept-level diagram of the RPC with a leading edge contamination control experiment. The experiment includes sample materials, contamination detection, jet spray and ion contamination removal devices and the AMCC to collect removed species. The experiment could be run autonomously or under remote control by shuttle or ground-based experimenters. The compactness, limited scope, simple design, and palletized nature of the experiment make it attractive for multiple RPC missions. (This Figure is an adaptation from reference 8.)